Earthquake Engineering, Tenth World Conference © 1992 Balkema, Rotterdam. ISBN 90 5410 060 5

Earthquake damage evaluation of reinforced concrete columns

J.Ogawa, J.Shibuya & M.Hoshi
Tohoku University, Sendai, Japan

Y.Abe
Tohoku Institute of Technology, Sendai, Japan

ABSTRACT : This experimental study, using large scale cantilever-type reinforced concrete column specimens, is aiming to investigate the biaxial lateral loading effect on strength and damage behavior of reinforced concrete columns. The strength degradation under biaxial loading paths is much more serious than that under uniaxial ones. Therefore, the biaxial loading gives more serious damage to concrete columns than the uniaxial loading. The biaxial loading with circular paths gives rise to more serious damage of concrete columns than that with linear paths. The cracking and spalling features of concrete columns under the biaxial loading are quite different from those of the uniaxial loading. The crack and spalling damage index from out side observation data of the damaged column can be applied for evaluating the damage state of reinforced concrete structures subjected to actual strong ground motions. According to this crack and spalling damage index, the crack length ratio reaches around 10, and the spalling area ratio reaches 10-30% at the drift angle of 1/70, triple of the yielding displacement.

1 INTRODUCTION

The seismic design criteria of structures in Japan is aiming at preventing structural damage due to moderate earthquakes, and avoiding collapse or serious structural damage due to severe and infrequent earthquakes. This concept means that some structures might be damaged to some extent, when they are subjected to severe earthquake excitations. It becomes very important to evaluate the degree of structural damage in structures so as to evaluate their post earthquake serviceability.

The biaxial lateral loading effect on strength and damage behavior of reinforced concrete columns is discussed. And the estimating method of the maximum displacement, experienced by concrete columns, is proposed from the relations between the displacement and the crack length ratio and the spalling area ratio, obtained from out side observation data of the damaged column such as cracking and spalling of concrete.

2 TEST SPECIMEN

Fig. 1 shows the cantilever-type column test specimen for biaxial lateral loading, used in this testing programs. Specimens are approximately full scale models, considered to be representative of the first story interior columns in typical three to five storied reinforced concrete buildings in Japan. The test specimens were cast in a vertical position in two batches, specimens BC-3 through BC-8 in the first batch, and BC-9 through BC-11 in the second. Table 1 shows the loading programs, the target displacements for each loading step, strengths of reinforcement and concrete, and the axial loads. Fig. 2 shows the loading setup for the biaxial test. The lateral load is applied at a height of 1,100 mm from the top surface of the footing block. The shear span ratio of this column is 2.2. The calculated ultimate flexural and shear strengths of specimens of BC-3 series are about 40.6 t and 41.9 t, respectively.

The column length of the specimen is shorter than the loading height of 1,100 mm, because the specimen needs to be attached at the free end of the column with the loading jig (height 490 mm), inducing the axial and lateral loads at the column top. For specimens BC-1 through BC-9, there was a loading height difference of 140 mm between the NS and EW axes, because two loading jacks in the mutually perpendicular directions had to be fit in the same center shaft of the jig. The loading height of 1,100 mm was measured from the center of the two loading axes to the top of the footing block. From specimen BC-10, the jig has been reformed to make two loading axes in the same height.

The lateral loading system is made up of two reversible hydraulic jacks (50t in both comp. and ten.). Both jacks are attached to the thick center shaft of the load inducing jig free joints in the vertical and horizontal directions at both ends. In each loading step, the test specimen is subjected to one cycle load reversals along the NS and EW directions, alternately or simultaneously. The lateral load, manually controlled, is adjusted to follow the prescribed displacement paths. The target displacement of each step is an integer multiple of the yielding displacement. The yielding displacement is

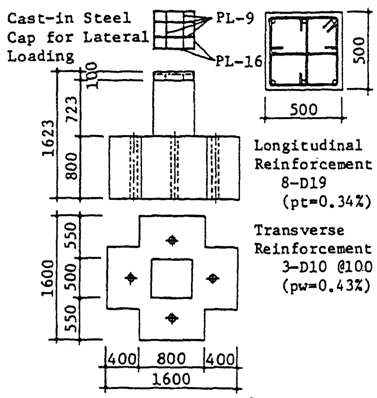

Fig. 1 Test specimen for biaxial loading

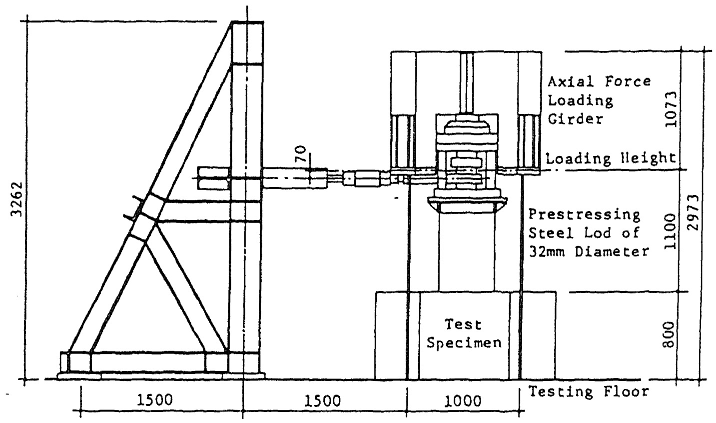

Fig. 2 Loading set-up for biaxial loading

Table 1 Test specimen, loading path and properties of materials

Spec.	Loading Program		Longitudinal		Transverse		Concrete		Axial Load (ton) (Ratio)
	Path	Steps ($R \times 10^{-2}$)	Bars	σ_y/σ_u (kg/cm²)	Bars	σ_y/σ_u (kg/cm²)	$_{28}F_c$ (kg/cm²)	test Fc (kg/cm²)	
BC - 1		0.5-1.5-2.5-5.0 [N.S-E.W]	8-D19 Pg=0.92% Pt=0.34%	3717 5331	3-D10 @100 Pw=0.43%	3845 5662	251	249	154.2(0.25)
BC - 2		0.25-0.5-1.5-2.5-3.5						280	157.0(0.25)
BC - 3		0.25-0.5-1.5-2.5-(3.5) [N.S-E.W]		3647 5552		3474 5150	274	248	171.3(0.25)
BC - 4		(5.0) [N.S-E.W]						249	173.1(0.25)
BC - 5		0.25-0.5-1.5-(2.5) [NE.SW-NW.SE]						254	171.8(0.25)
BC - 6		0.25-0.5-1.5-2.5-(3.5)						232	171.7(0.25)
BC - 7		0.5-1.0-1.5-2.0-2.5-3.5-(5.0) [N.S-E.W]						282	168.7(0.25)
BC - 8		0.5-1.0-1.5-2.0-2.5-3.5						286	172.0(0.25)
BC - 9		0.5-1.0-1.5-2.0-2.5-(3.5)		3668 5445		3449 5185	239	203	157.1(0.26)
BC - 10		1.0-1.5-2.0-2.5-3.5-5.0 [N.S]						192	157.5(0.26)
BC - 11		0.5-1.0-1.5-2.0-2.5-3.5-5.0						207	154.3(0.26)

In loading program column :
(5.0) : target displacement of uncompleted loading cycle
[N.S] : loading cycle in NS direction only
[N.S-E.W] : alternate loading cycles in NS and EW directions
[NE.SW-NW.SE] : alternate loading cycles in NE.SW and NW.SE directions

defined as the displacement, at which the tensile strain of the longitudinal reinforcement reaches or exceeds the target strain value of 0.2%. The yielding displacement occurs at a drift angle of around 1/200 rad.

The target axial load value is around 25 % of the axial ultimate strength, obtained by the product of the 28-day concrete strength and the gross sectional area of the column. The four hydraulic center hole jacks (100t in comp.) are used for the axial loading, and driven by the automatically controlled hydraulic pump.

3 INSTRUMENTATION

The column top displacements are measured at two points in each NS and EW direction, near the side edges of column surfaces, so as to eliminate the effect of horizontal twist of the column. Those four cylinder shaped displacement transducers were mounted to a stiff reference frame attached to the footing block, so that recorded displacements are relative to the footing. Both lateral and axial loads are measured by strain gage type load transducers, which are mounted to the loading jacks. The axial deformations of the column are measured along the two adjacent column surfaces by the strain gage type U-shaped or cylinder shaped displacement transducers with 100, 200 or 300 mm gage length. U-shaped transducers are fixed to the reference point bolts with thrust bearings in order to form rotation free joints. These bolts are firmly anchored in the core concrete. Strains of the longitudinal and transverse reinforcement are measured by 2 or 5 mm gage length foil strain gages with special water proof coating.

The displacements, loads, deformations, and strains are converted into electrical signals. During each cycle, the loading is temporarily stopped while the electrical signals are digitized and stored in a computer floppy disk. In addition, signals of the lateral displacements and lateral loads are displayed by digital volt meters, and recorded in a X-Y recorder for monitoring the loading paths and the response of the specimen.

Test specimens are whitewashed to make it easy to detect cracks on the concrete surfaces. Cracks, developed during loading, are marked with a pencil, so that crack patterns can be followed easily. When the residual displacement becomes zero at the end of each loading step, crack patterns and outlines of concrete spalling area are traced with a fiber tip pen on a transparent thin plastics sheet of 500 mm width. The width of the sheet is made equal to that of the column, so as to make it easy to reset the plastic sheet as required, when tracing cracks and spalling. Cracks and outlines of the concrete spalling area are divided into small linear segments at adequate intervals by manual operation. Vector data of these linear segments are obtained by a tablet digitizer and stored in a computer floppy disk. The cracks at the corner between the column face and the top of the footing block are not traced.

After setting a computer display to 500 pixels representing the column width of 500 mm, crack patterns are drawn with blue lines on the computer display, using vector data of crack patterns. If concrete spalling data exist, outlines of the spalling area are drawn with red lines on the same display. The inside of the spalling figure is painted red, in order to delete crack patterns included in the figure as hidden line elimination. The total crack length is obtained by counting up the number of the blue pixels indicating the crack patterns. The total spalling area is obtained by counting up the number of the red pixels indicating the spalling areas.

4 TEST RESULTS & DISCUSSION

4.1 *Damage*

Fig. 3 shows the crack pattern and the spalling area of specimen BC-6 at the end of each loading step. Horizontal cracks become visible in all surfaces at a drift angle of 1/400. As the drift angle increases to 1/200, mainly horizontal cracks continue to develop together with a few diagonal cracks. The cracks at the bottom parts continue to increase and expand as the displacement of the column increases up to a drift angle of 1/70. Beyond a drift angle of 1/70, the rate of development of new cracks slows down, some existing cracks are seen to widen further, and shallow concrete spalling begins in surfaces. At a drift angle of 1/40, concrete cover spalling occurs over wide area on all surfaces, and the reinforcement is uncovered. Some of the longitudinal reinforcement buckle slightly between transverse reinforcement. At a drift angle of 1/30, the core concrete,

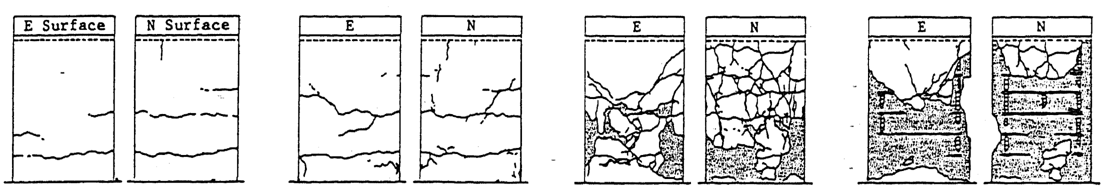

Fig. 3 Crack pattern and spalling of specimen BC-6 at end of loading steps

confined with crossties and transverse reinforcement, disintegrates seriously. This leads to opening of end hooks (135 or 180 deg.) of crossties and transverse reinforcement, so that the concrete core is no longer confined. The column length becomes rapidly shorter under the action of axial load with the consequent large scale buckling of longitudinal reinforcement.

4.2 *Hysteresis loops*

Fig. 4 shows load displacement hysteresis loops of specimen BC-6, as a typical representative of specimens under the biaxial loading. Specimen BC-6 is subjected to the areal biaxial loading with circular paths, so the load displacement hysteresis loops are independently drawn as projected charts on the NS (solid line) and EW (dotted line) load displacement planes. The envelope curve of specimen BC-6 reaches the ultimate strength at a drift angle of around 1/100. After the ultimate strength, hysteresis loops show very rapid strength degradation. Specimen BC-6 shows more serious strength degradation than any other specimens. Fig. 4 also shows the load displacement relation of specimen BC-4 (broken line), subjected to big one cycle loadings up to a drift angle of 1/20. The load was applied firstly along the NS axis, and then along the EW axis. The specimen collapsed half way through the EW loading. It can be said that the biaxial loading gives much severer damage on the column than the uniaxial loading. The areal biaxial loading with the circular paths give severer damage than the linear biaxial loading with alternative cross paths.

4.3 *Crack ratio and spalling ratio*

The equivalent crack length is calculated on the square area (500 x 500 mm^2) of one column width sides at the bottom of the column by the pixel counting method, mentioned above. The crack length ratio is defined as

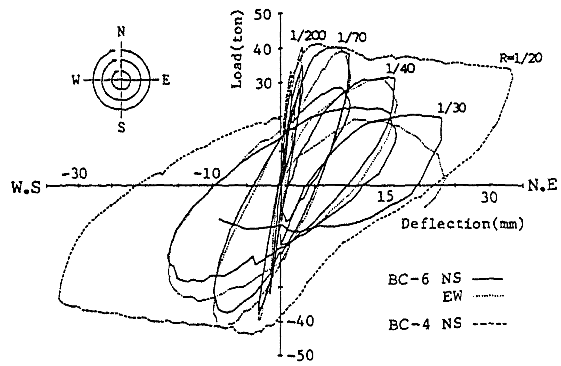

Fig. 4 Load displacement hysteresis loops of specimens BC-6 and BC-4

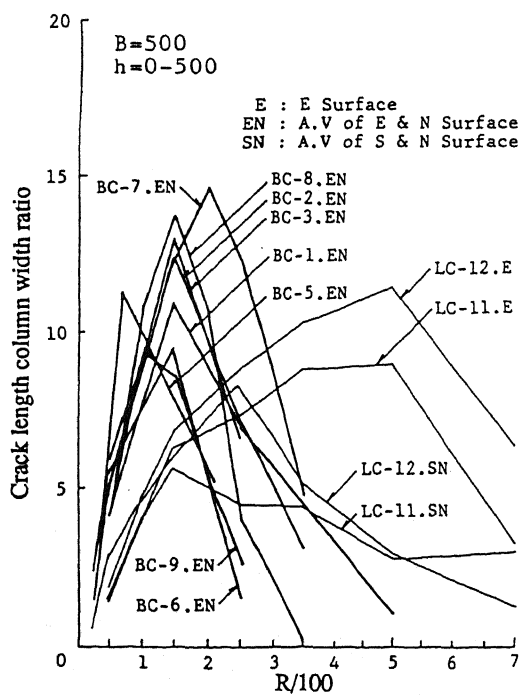

Fig. 5 Crack length ratio and drift angle

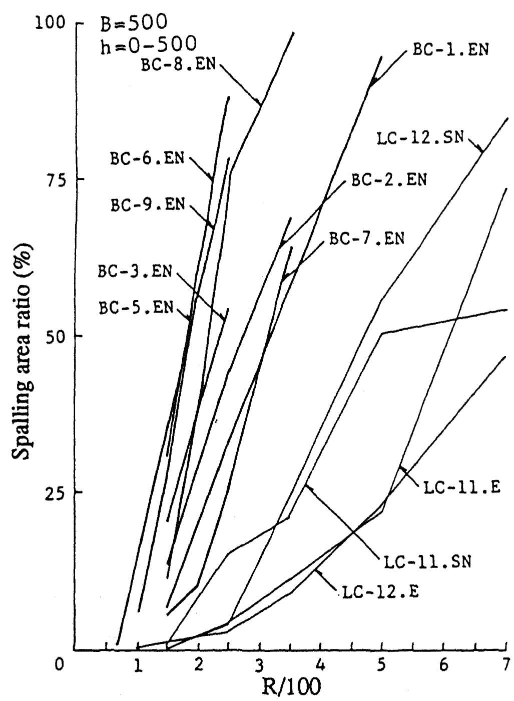

Fig. 6 Spalling area ratio and drift angle

the ratio of the total crack length to the column width. Fig. 5 shows the relations between the crack length ratio and the drift angle for both the uniaxial and biaxial loading cases. For the biaxial case, the crack length ratio is seen to increase with the drift angle up to a value of 1/70. After that, the crack length ratio decreases rapidly due to concrete spalling. At a drift angle of 1/200, the crack length ratio is about 5. At a drift angle of 1/70, the ratio becomes about 10.

The total concrete spalling area is calculated on the same square area and the same method as the crack length is calculated. The spalling area ratio is defined as a percentage of the spalling area to the whole target area. Fig. 6 shows the relations between the spalling ratio and the drift angle for both the uniaxial and biaxial cases. The spalling ratio increases rapidly with the increment of the drift angle from a value of 1/70.

It is to be noted that the crack ratio and the spalling ratio used in this study are the relative values for expressing the level of earthquake damage. The crack and the spalling ratios for the biaxial loading cases should be used for evaluating the earthquake damage of reinforced concrete buildings which have almost same deformation characteristics in both the longitudinal and transverse directions. The information on the crack width is not considered here.

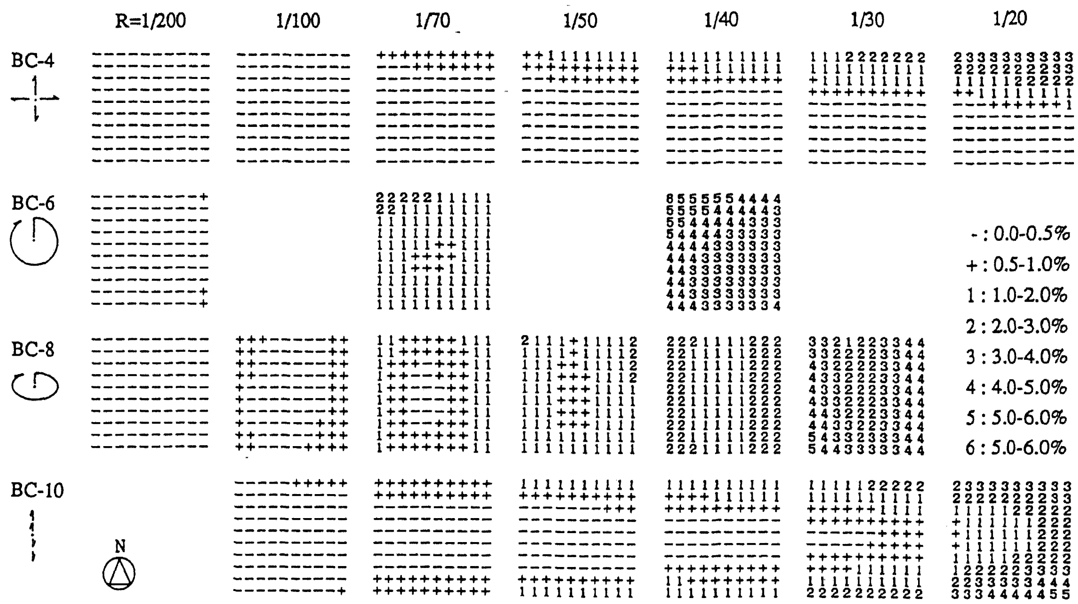

Fig. 7 Strain distribution in cross section (0-300 mm)

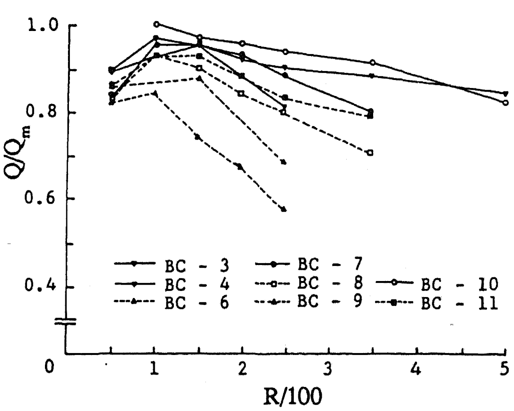

Fig. 8 Maximum drift angle and strength ratio

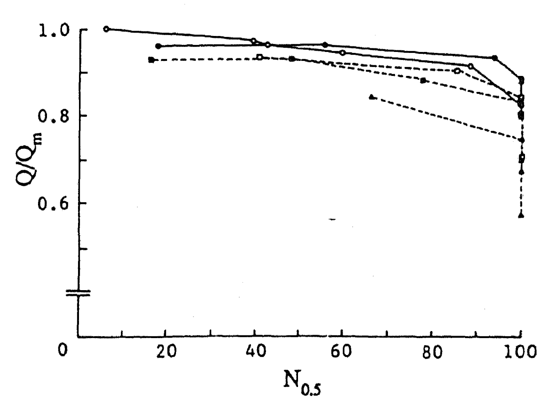

Fig. 9 0.5% strain elements and strength ratio

4.4 *Strain distribution in cross section*

The strain distribution of the column cross section was calculated from four data of the axial deformation of the 0-300 mm range from the top surface of the footing block by the least mean square method, using conventional assumption that plane sections remain plane. Therefore, these strain values are the average values along the 300 mm measuring length.

Fig. 7 shows the representatives of the strain distribution in the cross sections, indicated by the strain step wise values of the 10x10 subdivided rectangular sectional elements. The strain values of each element indicate the maximum compression strain, experienced during each loading step.

The value and distribution of the strain by the biaxial cases are quite different from those of the uniaxial cases. At the same drift angle, the biaxial loadings give higher strain values and wider high strain area than the uniaxial ones. At a drift angle of 1/70, the strain of only 40% of sectional elements exceeds 0.5% compression strain in the uniaxial loadings, but those of 100% of them exceeds 0.5% strain in the circular biaxial ones. In the uniaxial loadings, the strain of 100% of the elements exceeds 0.5% strain at a drift angle of 1/20.

4.5 *Strength ratio*

The standard ultimate strength (45.0t) for the first batch, specimens BC-3 through BC-8, was obtained from the average value of the ultimate strengths in the N and S directions of specimen BC-4, subjected to 1/20 drift angle big one loops loading. That (42.8t) for the second batch, BC-9 through BC-11, was obtained from the test results of the BC-10, step wise cyclic reversals uniaxial loadings. The strength ratios were defined as the ratio of the strengths of the specimen at the time to the standard ultimate strengths.

The strength values of specimens BC-3 through BC-9 were corrected to the equivalent strength values of the nominal loading height of 1,100 mm, because of the loading height differences of 70 mm longer in the NS direction and 70 mm shorter in the EW direction than the nominal loading height.

4.6 *Drift angle and strength ratio*

Fig. 8 shows relations between the maximum experienced drift angle of the column and the strength ratio. This figure indicates the type of loading paths affects this relation, significantly. After a drift angle of 1/100, when the almost all specimens reached the ultimate strengths, the strength reduces with the increment of the drift angle. The strength degradation is very slight in the uniaxial loadings. The degradation is quite severe in the areal biaxial loadings with circular paths. In the linear biaxial loadings with alternate cross paths, the degradation is in between those extreme cases. At a drift angle of 1/40, the strength ratio is around 0.9 in the uniaxial loading, around 0.8 in the linear biaxial loading but around 0.65 in the circular biaxial loading. The specimens could carry the axial load up to a drift angle of 1/20 in the uniaxial loading, 1/30 in the linear biaxial loading, and 1/40 in the circular biaxial loading.

4.7 *Compression strain and strength ratio*

Fig. 9 shows relations between the percentage of the number of the 0.5% or more compression strain elements in the column cross section and the strength ratio. When all elements in the cross section experienced 0.5% or more compression strain, the strength ratio reduced to 0.85. The column cross section gets this condition at a drift angle of 1/20 in the uniaxial loadings, 1/30 in the linear biaxial ones and 1/40 in the circular biaxial ones. After this condition, the axial deformation of the column increased very rapidly with the increment of the column top displacements.

5 CONCLUSIONS

Because of limited number of test specimens and limited cases of loading programs, further researches are needed, but major conclusions include the following:

1. The biaxial loadings give more serious damage to the concrete columns than the uniaxial ones. The circular biaxial loadings give rise to much more serious damage to the concrete columns than the linear ones. At a drift angle of 1/40, the strength ratio becomes 0.9 in the uniaxial loading, and 0.6 in the biaxial one. The biaxial loading effects should be taken into account for the modeling of restoring force characteristics of structures in biaxial loading condition.
2. The values and the distributions of the high compression strain in the column cross section show the state of damage of the columns. When the cross section experienced 0.5% or more compression strain, the strength ratio becomes less than 0.85. The columns of the biaxial cases reach at smaller displacement than those of the uniaxial cases.
3. According to the crack and spalling damage index, the following observations can be made:
   a) If the crack length ratio is around 5, the maximum drift angle is less than 1/200.
   b) If the crack ratio is around 10 and the spalling area ratio is 10-30 %, the drift angle is around 1/70.
   c) If the spalling ratio is 30-85 % and reinforcing bars are uncovered due to concrete cover spalling, the drift angle is around 1/40.
   d) If the spalling ratio is more than 50 %, transverse bars become loose and longitudinal bars buckle, the drift angle is over 1/40.